



Article

Conceptual Design of Seismic Retrofit of Existing Bridges by Deck Isolation: Assessment of Effectiveness

Carlo Pettoruso  and Virginio Quaglini * 

Department of Architecture, Built Environment and Construction Engineering, Politecnico di Milano, Piazza Leonardo da Vinci 32, 20133 Milan, Italy; carlo.pettoruso@polimi.it

* Correspondence: virginio.quaglini@polimi.it; Tel.: +39-02-23994248

Featured Application: A simple and fast tool is proposed for assessing the rehabilitation needs of bridges and the effectiveness of implementing the seismic isolation of decks to reduce the vulnerability of bridges.

Abstract: The creation of an isolation layer between decks and substructures has turned out to be a viable method for reducing the seismic vulnerability of existing bridges. However, to the Authors' knowledge, a practical approach for a preliminary verification of the effectiveness of this intervention is lacking. The paper introduces a practical tool for a preliminary assessment of the needs of the rehabilitation of the bridge and of the effectiveness of the deck isolation to improve its seismic performance by comparing the demands of the as-built structure and of the piers alone, expressed in terms of equivalent accelerations, to the maximum seismic acceleration allowed to maintain the substructure behavior in the elastic range. A practical implementation of the criterion is illustrated in a parametric study, considering prototypes of simply supported and continuous deck bridges with features common to the bridges of the Italian stock. The results of the study provide some indications about the inherent weaknesses of the examined pier typologies and the positive effect of the dead load of the deck on the effectiveness of deck isolation.

Keywords: bridges; retrofit; seismic isolation; ground motion; simplified analysis; preliminary assessment; equivalent acceleration



Citation: Pettoruso, C.; Quaglini, V. Conceptual Design of Seismic Retrofit of Existing Bridges by Deck Isolation: Assessment of Effectiveness. *Appl. Sci.* **2024**, *14*, 7353. <https://doi.org/10.3390/app14167353>

Academic Editor: Asterios Bakolas

Received: 16 July 2024

Revised: 30 July 2024

Accepted: 7 August 2024

Published: 20 August 2024



Copyright: © 2024 by the authors. Licensee MDPI, Basel, Switzerland. This article is an open access article distributed under the terms and conditions of the Creative Commons Attribution (CC BY) license (<https://creativecommons.org/licenses/by/4.0/>).

1. Introduction

The rehabilitation of existing constructions has been gaining increasing interest in recent years for its huge impact on the socio-economic system. The subject has been deeply investigated for buildings, leading to the formulation of rehabilitation strategies that have now been incorporated into design codes [1–3], but comparable development for bridges and viaducts is still lacking. In particular, although deck isolation, achieved by creating an isolation layer between the deck and the substructures, has proven to be a viable method for reducing the seismic vulnerability of bridges [4,5], a survey of the state of the art shows that, to date, only a few codes of practice have been published regarding the application of seismic isolation for bridge retrofitting, despite the widespread use of this technique over the last three decades [6–8].

Some approaches for the conceptual design of seismically isolated bridges (which can be extended to the retrofit of bridges by simply replacing the existing bearings with isolation systems), have been formulated in the past by different Authors. In 1997, Calvi and Pavese [9] proposed a displacement-based design procedure that uses a single-degree-of-freedom equivalent linear model of the bridge. The design process begins by defining the maximum displacement allowed during the design earthquake, which is then applied uniformly to all piers and abutments (assuming a perfectly regular structure). The yield displacement of each pier is calculated by integrating the curvature along the height of

the column and assuming proportionality between the moment and curvature. The actual displacement of each isolator is determined by requiring that the force at the target displacement does not exceed 85% of the yield force of the pier, and the isolator's yield displacement is calculated by dividing the actual displacement by the isolator ductility, chosen by the designer in order to prevent collapse during extreme events. The effective ductility of the equivalent single-degree-of-freedom (SDOF) isolated bridge is determined as the ratio between the maximum allowed displacement and the sum of the yield displacements of the isolators and the piers. Subsequently, the equivalent viscous damping ratios of the isolation system and the structure are defined. Using the displacement spectrum for the appropriate equivalent damping ratio, the period of the first vibration mode is calculated, thus obtaining the equivalent stiffness of the isolated bridge. Then, the procedure ends with the determination of the stiffness of the isolation system. After presenting the procedure for the design of new bridges, the Authors briefly discuss its application to existing bridges, highlighting two main problems, namely, the different response of the bridge in the two directions and the possible presence of weaker structural elements. This procedure was subsequently extended by Jara and Casas [10] to the case of bridges supported by isolators with a bilinear hysteretic loop, such as lead rubber bearings, taking into account the contribution of the bearings to the equivalent viscous damping of the system. An iterative procedure in nine steps was presented, but its application was conceived for new bridges only.

Dolce et al. [11] addressed the design of isolation systems with bilinear force-displacement behavior, represented by flat sliding bearings combined with recentering devices and considering three different devices: rubber springs, steel springs, and shape memory alloys, respectively. Two iterative procedures were developed to design the isolation system, the design displacement approach, and the design force approach. Both procedures are based on the Capacity Spectrum Method (CSM), as defined in ATC 1996 [12]: the CSM compares the capacity curve of the structure, represented by a multilinear force-displacement relationship, with a damped response spectrum representing the seismic demand; the intersection of the two curves identifies the performance point, which defines the maximum global response expected during the ground motion. In the design force approach, the goal is to limit the maximum force transmitted by the isolation systems to an assigned percentage of the pier's yield strength, while in the design displacement approach, the goal is to limit the maximum displacement of the isolation systems to a percentage of its ultimate displacement capacity. The iterative process involves adjusting the maximum displacement or maximum force of the isolation systems, which in turn affects the effective period and the overall damping of the system, until convergence is achieved.

Cardone et al. [13] developed a design procedure which takes into account five different cyclic force-displacement behaviors of the isolation system, namely, viscoelastic, elastic-plastic with hardening, rigid-plastic with hardening, double-flag-shaped, linear, or nonlinear viscous behavior. At the beginning of the procedure, the designer assigns the displacement of the isolation system in each direction, considering the characteristics of the selected isolator type. During the design phase, the maximum displacements of the piers and of the joints are verified to ensure that they are lower than the relevant yield displacements and the available clearances, respectively. The choice of the isolation system is linked to the amount of damping that the designer wants to obtain. For this purpose, the Authors developed a graphical procedure, valid for both existing and new bridges. The principle consists in plotting the yield point of the equivalent SDOF bridge on the ADRS plane, along with damped demand spectra for various damping values associated with the different types of isolators. Once the damping is chosen, an iterative procedure is then performed to define the optimal stiffness of the isolator that achieves the target displacement in both directions.

Xie and Zhang [14] developed a system-level repair cost ratio design surface for various base-isolated bridges, facilitating performance-based design and device optimization. The methodology is based on the derivation, for bridges with different isolation systems, of

component fragility surfaces as functions of multiple engineering demand parameters. The system-level repair cost ratio surface is derived by incorporating the damage probabilities, damage ratios, and replacement costs of bridge components. Subsequently, the uniform repair cost ratio function is used as a performance index, and a genetic optimization procedure is implemented to obtain the mechanical properties of isolation systems that lead to the lowest repair cost ratio.

Furinghetti and Pavese [15] presented a simplified procedure for the isolation of a continuous reinforced concrete (RC) bridge girder. The goal is to simplify the determination of isolator response parameters and the definition of an optimal layout based on predefined structural performance criteria.

Wei et al. [16] proposed an equivalent energy-based design procedure to improve the seismic performance of high-speed railway (HSR) bridges by using friction pendulum bearings (FPBs). The procedure balances the total input seismic energy with energy dissipation and deformation capacity, providing a holistic approach to the structural response. The method offers simpler calculations compared to traditional methods, but it is strictly related to the characteristics of the Chinese HSR, for which it was developed. Gkatzogias and Kappos [17] proposed a procedure based on the Deformation-Based Design method. It introduces four performance levels, depending on the importance of the bridge and the consequences of the failure (effect on human life; short- and long-term economic effects of service disruption; repair and replacement costs). Generalized design equations aid in the early identification of critical performance levels and the selection of optimal designs with minimal computational effort, eliminating the need for iterative analyses.

As highlighted in the brief overview, most of the cited studies were developed for specific technologies of the isolation system and therefore may not have general validity. Furthermore, most approaches require iterative procedures to account for the inherently non-linear response of isolation systems with high damping capacity, such as High Damping Rubber Bearings, Lead Rubber Bearings, and the Friction Pendulum system. Additionally, in the case of existing bridges, a preliminary analysis of the actual rehabilitation needs of the bridge, to verify that isolation is effective in reducing the vulnerability of the structure, is usually not performed. The Authors of this paper formulated a new conceptual approach for the seismic retrofitting of existing bridges using seismic isolation. The retrofit is implemented by isolating the deck from the substructures, by replacing the bridge bearings with seismic isolators, and is applied to bridges characterized by a static scheme of either a simply supported deck or continuous deck on multiple supports, where the deck rests on conventional bridge bearings. These static layouts appear to be the most widespread in the Italian panorama, where they represent over 90% of existing bridges [18,19]. The retrofit, in line with current code provisions [20–22], aims at keeping the behavior of the substructures elastic during the design earthquake. The method consists of two phases: (i) the assessment of the effectiveness of deck isolation in reducing the bridge vulnerability, given the characteristics of the bridge and the seismic scenario, and (ii) the determination of the effective stiffness and effective damping of the isolation system to achieve the specified performance of the retrofitted structure. The procedure is in principle applicable to all technologies of isolation systems, and only after the definition of the mechanical properties of the isolators is it possible to choose the most effective devices from the catalogues of the manufacturers.

This paper is dedicated to illustrating the first part of the method, which consists of assessing the effectiveness of the deck isolation to reduce the vulnerability of the bridge, while the preliminary design of the isolation system will be the subject of a future study. After introducing the criterion of effectiveness, a parametric study is developed considering different bridge prototypes obtained by varying the geometry of the piers and the type of deck. The bridge prototypes are analyzed for different sites, highlighting how various parameters affect the effectiveness of the isolation retrofit.

2. Formulation of the Effectiveness Criterion

The effectiveness criterion is formulated with the aim of providing a tool for a preliminary assessment of the effectiveness of the seismic retrofit of the existing bridge by creating an isolation layer between the deck and the substructures. The goal of the retrofit is to reduce the seismic force associated with the mass of the deck and obtain an essentially elastic behavior of the substructures during the design earthquake, in accordance with code requirements for isolated structures [20–22]. The feasibility of the intended retrofit is subjected to the presence of conventional bridge bearings between the deck and the substructures and, consequently, to the static scheme of the deck.

The procedure is represented schematically in the flow chart in Figure 1 and is described step-by-step in the following sub-sections. To define the main components of the bridge, refer to Figure 2.

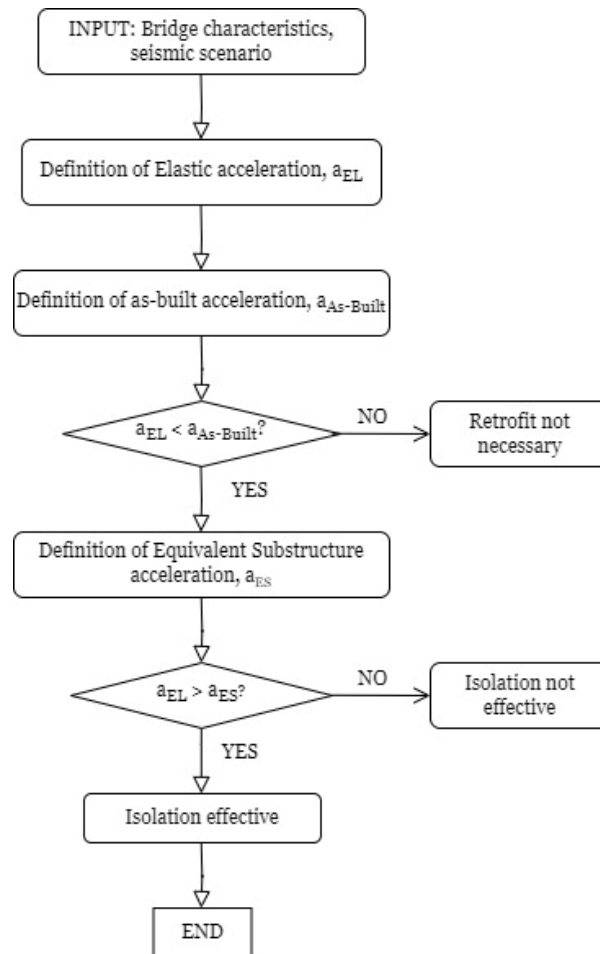


Figure 1. Flow chart for the assessment of the effectiveness of deck isolation.

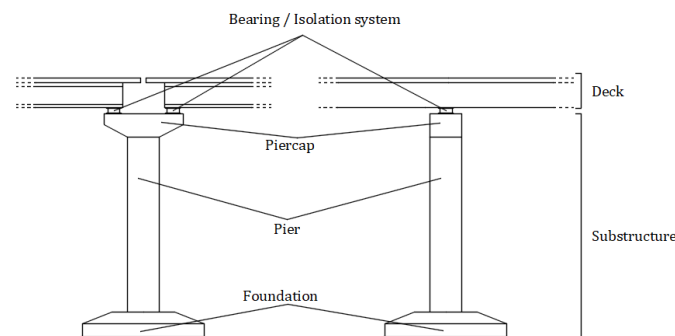


Figure 2. Nomenclature of the bridge’s main components.

2.1. Input: Bridge Characteristics and Seismic Scenario

The first step consists of collecting the geometrical and material characteristics of the bridge, including

- The masses of the bridge elements, grouped in the mass of the deck (m_{deck}), the mass of the piers (m_{pier}), and the mass of the pier caps ($m_{piercap}$);
- The properties of the pier materials: the modulus of elasticity and characteristic compressive strength of concrete (E_c, f_{ck}) and the modulus of elasticity and characteristic yield strength of steel reinforcement (E_s, f_{yk});
- Geometric properties of the piers (cross-sectional area A and area moment of inertia I ; height of the column);
- Details of the steel reinforcement in reinforced concrete (RC) piers;
- Bearing layout.

The mass of the deck includes the mass of both structural and non-structural components such as the slab, beams, parapets, lights, etc. The material and geometric properties are those required for evaluating the stiffness of the piers. It is worth noting that the same information will be needed for the design of the isolation system in the second phase of the method [23]. Information can be retrieved from the bridge documentation (design report, drawings, etc.), if available, or from site inspection and structural tests for geometric and mechanical properties, respectively.

The assessment of effectiveness is performed by studying a simplified model, or “elementary bridge unit”, which represents a single pier of the bridge, its pier cap, and a section of the deck with assigned mass (c) depending on the tributary loading area of the pier itself. Starting from this simplified physical model, an equivalent SDOF model of the elementary bridge unit is formulated (Figure 3).

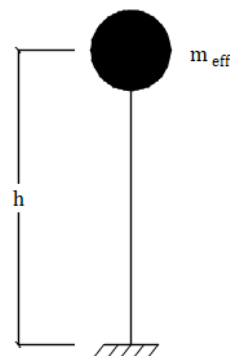


Figure 3. Equivalent SDOF of the elementary bridge unit: m_{eff} = effective mass; h = height.

In accordance with the Italian Building Code, IBC [20], §7.9.4.1, the effective mass of the elementary bridge unit is defined as the sum of the masses of the deck section, the pier cap and the upper third of the pier:

$$m_{eff} = m_{deck} + m_{piercap} + m_{pier}/3 \quad (1)$$

where the seismic mass of the deck m_{deck} includes masses of structural elements (m_{g1}) and nonstructural elements (m_{g2}), plus the mass relating to the traffic loads multiplied by the participation factor $\psi_2 = 0.2$ ($m_{0,2q}$), according to IBC [20], §2.5.3 and §5.1.3.12:

$$m_{deck} = m_{g1} + m_{g2} + m_{0,2q} \quad (2)$$

The loads transmitted from the superstructure to the piers depend on the static scheme of the bridge.

For simply supported bridges, the bearing layout provides, for each span of the deck, a pinned axis (the bearings can rotate around the transversal axis of the bridge but do not allow for displacement) and a rolling axis (the bearings can rotate around the transversal

axis and move longitudinally). Therefore, the seismic mass acting on the single pier, in the longitudinal direction, is the mass of the span connected to the pier via the pinned axis. In the transverse direction, it is assumed that the displacements of both axes are constrained, and therefore, the seismic mass acting on the pier is equal to half the mass of each span supported on the pier.

For continuous deck bridges, the mass distribution on the piers is also affected by the stiffnesses of the piers and the deck and in principle can be evaluated through an elastic analysis that considers these properties. However, to simplify the assessment, the bridge mass can be assumed as distributed over the piers according to the concept of the tributary loading area. The adequacy of this assumption for a continuous deck is demonstrated in reference [23] and in Appendix A of this paper.

2.2. Definition of Elastic Acceleration a_{EL}

The capacity of the pier is defined in terms of the first yield moment, M_y , and shear strength, V_{RD} , which characterize the ductile or brittle failure mechanisms, respectively. In calculating the moment at first yield, the effect of the axial load at the base of the pier associated with the seismic masses of the deck and pier is taken into account.

Considering the equivalent SDOF model of the elementary unit of the bridge (Figure 4), the structural accelerations that trigger both collapse mechanisms can be calculated as follows.

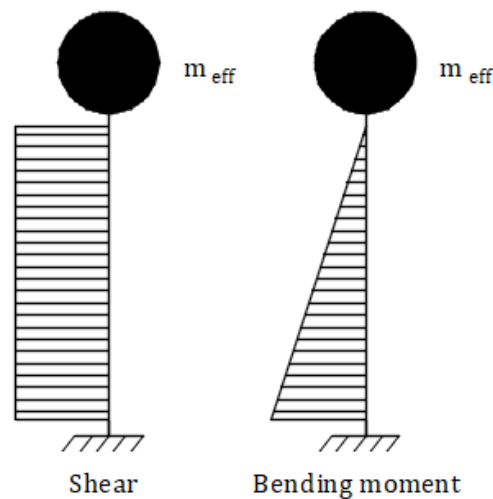


Figure 4. Internal forces in the elementary bridge unit for shear and bending.

Considering the equivalent SDOF model of the elementary bridge unit (Figure 4), the structural accelerations the trigger both collapse mechanisms can be calculated as follows:

$$a_{bending} = \frac{M_y}{h \cdot m_{eff}} \tag{3a}$$

$$a_{shear} = \frac{V_{RD}}{m_{eff}} \tag{3b}$$

The minimum between these two accelerations defines the “Elastic Limit acceleration”, i.e., the maximum ground acceleration for which the piers maintain elastic behavior and which constitutes the target of the seismic retrofit:

$$a_{EL} = \min(a_{bending}, a_{shear}) \tag{4}$$

2.3. Definition of As-Built Acceleration $a_{As-Built}$

By analyzing the equivalent SDOF model of the elementary bridge unit through equivalent static analysis, the spectral acceleration of the as-built structure, or “As Built

acceleration", can be determined from the relevant mass and stiffness. The bending stiffness of the pier is

$$K = \frac{3EI}{h^3} \quad (5)$$

where E is the effective modulus of elasticity and I is the area moment of inertia of the pier, and the corresponding period is

$$T_{As-Built} = 2\pi\sqrt{m_{eff}/K} \quad (6)$$

Given the period, the As-Built acceleration $a_{As-Built}$ is obtained from the 5%-damped elastic spectrum of the site.

2.4. First Condition: Retrofit Need

The As-Built acceleration represents the seismic demand on the elementary bridge unit given the stiffness of the pier and the spectral characteristics of the site. Comparing the As-Built with the Elastic Limit acceleration, two scenarios can occur:

1. the As-Built acceleration is smaller than the Elastic Limit acceleration; this means that the seismic demand is smaller than the capacity of the pier, and retrofit is unnecessary.
2. the As-Built acceleration is larger than (or equal to) the Elastic Resource acceleration; in this case, the pier is unable to withstand the seismic force associated with the supported mass of the deck, and the isolation of the deck can represent a valid solution for reducing its vulnerability.

The first condition (retrofit need) is hence defined as

$$a_{EL} \leq a_{As-Built} \quad (7)$$

The check must be performed in the two principal directions of the bridge, longitudinal and transversal. The retrofit of the bridge is needed if condition (7) is met in at least one direction.

If the bridge has a regular layout, with uniform spans and cross-sections, and the piers all have the same geometry (cross-section and height) and materials, it is sufficient to verify the inequality (7) for a single elementary bridge unit. Otherwise, it is necessary to define an equivalent SDOF model for each different pier geometry and/or span length and repeat the verification for the corresponding elementary bridge unit.

2.5. Definition of Equivalent Substructure Acceleration a_{ES}

Deck isolation is implemented by replacing the bridge bearings with seismic isolators and creating an isolation layer between the deck and the substructures. According to this layout, the isolation is effective in reducing the acceleration of the deck but has no effect on the acceleration of the masses beneath the isolation layer. Therefore, it is necessary to evaluate whether the capacity of the piers is sufficient to resist the seismic force associated with their own masses.

In accordance with IBC [20], §7.9.4.1, the mass of the not-isolated substructure is defined as the mass of the pier cap and one-third of the mass of the pier:

$$m_{sub} = m_{piercap} + m_{pier}/3 \quad (8)$$

Assuming that the deck is completely isolated, the substructure can be studied on its own. The effective period of the substructure is

$$T_{sub} = 2\pi\sqrt{m_{sub}/K} \quad (9)$$

where K is the stiffness of the pier calculated according to Equation (5).

Given the period, the substructure acceleration a_{sub} is obtained from the 5%-damped response spectrum.

Referring to the three accelerations introduced so far, namely, a_{EL} , $a_{As-Built}$, and a_{sub} , the associated seismic forces can be written as

$$V_{EL} = a_{EL} \cdot m_{eff} \quad (10a)$$

$$V_{As-Built} = a_{As-Built} \cdot m_{eff} \quad (10b)$$

$$V_{sub} = a_{sub} \cdot m_{sub} \quad (10c)$$

To compare the accelerations in the same space, it is necessary to refer them all to the same mass. Therefore the “Equivalent Substructure acceleration” is introduced:

$$a_{ES} = \frac{a_{sub} \cdot m_{sub}}{m_{eff}} \quad (11)$$

2.6. Second Condition: Isolation Effectiveness

The relationship between the seismic force acting on the not isolated substructure and the elastic capacity of the pier is expressed, in terms of spectral acceleration, by comparing the Equivalent Substructure acceleration with the Elastic Limit acceleration. From this comparison, the second condition (isolation effectiveness) follows:

$$a_{ES} \leq a_{EL} \quad (12)$$

Inequality (12) expresses the fact that, if a_{ES} is less than or equal to a_{EL} , then the elastic capacity of the pier is sufficient to resist the seismic force associated with the not isolated mass of the pier. Unlike Inequality (7), Inequality (12) must be satisfied in both principal directions of the bridge; otherwise, deck isolation alone is not effective in reducing the vulnerability of the structure, and other approaches must be implemented, such as local strengthening, etc.

By combining Inequalities (7) and (12), the criterion of effectiveness for deck isolation can therefore be formulated as

$$a_{ES} \leq a_{EL} \leq a_{As-Built} \quad (13)$$

This criterion is graphically represented in Figure 5.

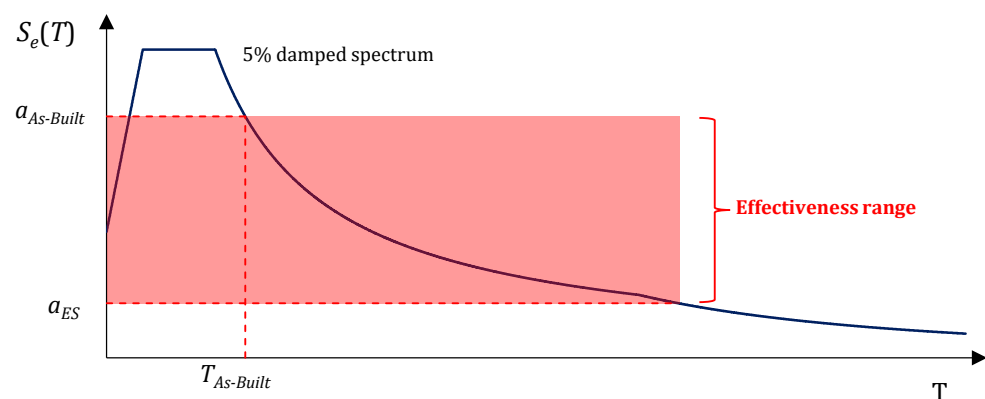


Figure 5. Graphical representation of the effectiveness criterion: a_{EL} must fall in the colored band between $a_{As-Built}$ and a_{ES} .

3. Parametric Study

In order to show how the criterion allows for assessing whether the upgrading of the bridge is necessary and whether the deck isolation alone is effective in reducing the bridge vulnerability, a parametric study was developed, analyzing different cases in terms of static

schemes, the sectional characteristics and height of the piers, the mass of the deck, and the seismic scenario. The bridge prototypes analyzed in the study were defined by referring for convenience to common characteristics of the Italian bridge stock, but the general validity of the method is not affected by the actual bridge characteristics, provided that the bridge deck is supported by bridge bearings.

3.1. Static Scheme

Two static schemes are examined, namely, the simply supported deck and the continuous deck on multiple supports.

The two schemes can be implemented in practice by different bearing arrangements, especially in seismic conditions. The assumed layouts and their implications in terms of seismic mass distribution from the deck to the pier are described below.

3.1.1. Simply Supported Scheme

The simply supported bridges considered in the study have four spans of uniform dimensions and masses, supported by two abutments and three piers. In the longitudinal direction, each span has a pinned axis at one end and a movable axis with rollers at the other end, as shown in Figure 6; in the transverse direction, both ends are restrained. According to this scheme, in the longitudinal direction, the seismic mass acting on each pier is the mass of the span with the pinned connection; in the transverse direction, the seismic mass on the pier will be given by the sum of half of the seismic mass of both supported spans. Considering spans of the same length and cross-section, the seismic masses acting in the longitudinal direction and in the transversal direction are the same.

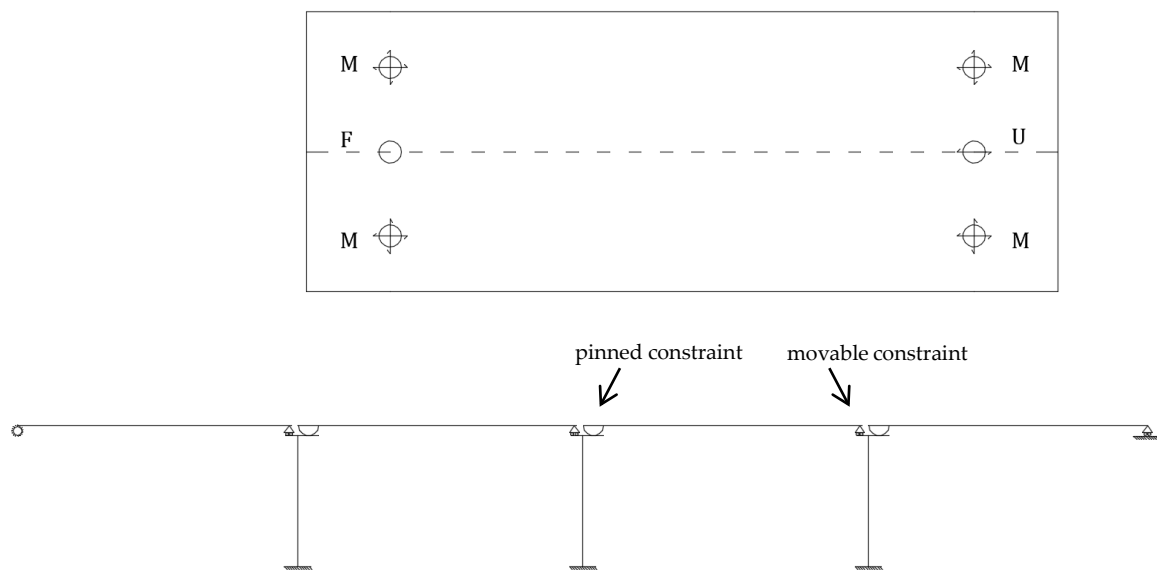


Figure 6. Static scheme for simply supported bridges. M = Multidirectional bearing; U = Unidirectional bearing; F = Fixed bearing.

Three configurations of simply supported bridges, characterized by different heights of the three piers, are included in the study:

- 5 m–5 m–5 m;
- 10 m–10 m–10 m;
- 20 m–20 m–20 m.

3.1.2. Continuous Deck Scheme

Bridges with continuous deck bridges supported by two abutments and three piers are considered, with spans of uniform length. The presence, on all piers and abutments, of seismic restraints is assumed, as shown in Figure 7a, so that during the ground motion,

the seismic force of the deck is shared among all substructures. This bearing layout is quite common in the Italian stock of railway bridges [24]. The alternative layout, shown in Figure 7b, with fixed bearings on an abutment and movable bearings on all piers and the second abutment, is not considered in the study since abutments are generally rigid elements with a high load bearing capacity, and seismic retrofitting would probably not be necessary.

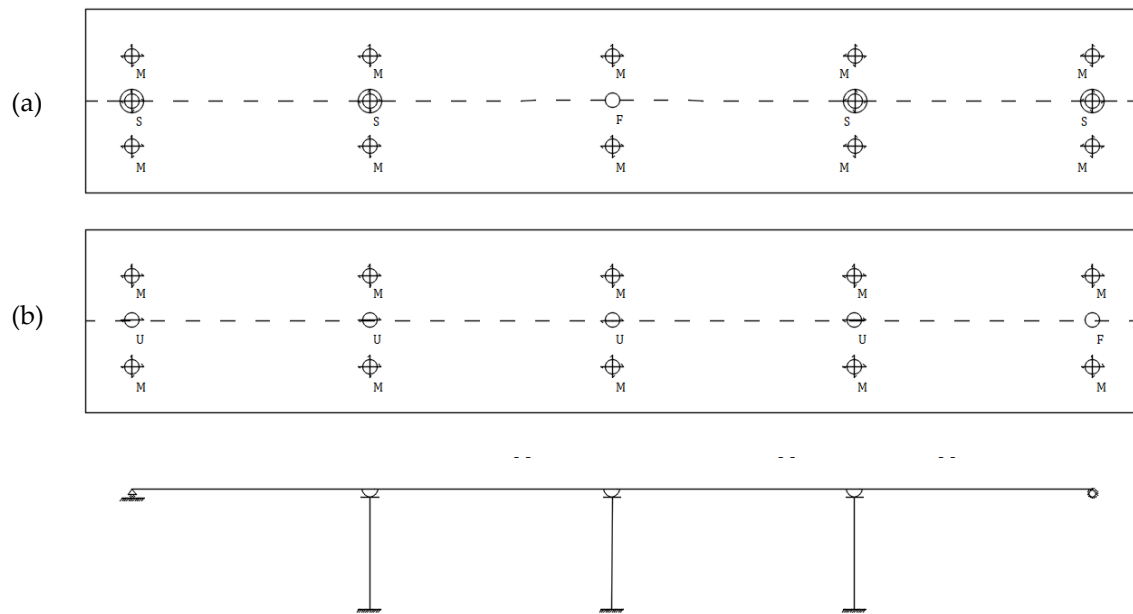


Figure 7. Bearing layouts for continuous deck bridges: (a) with seismic restraints on each axis; (b) with fixed constraints on one abutment. M = Multidirectional bearing; U = Unidirectional bearing; F = Fixed bearing; S = Seismic restraint engaged during the ground motion.

The vertical reactions on piers and abutments depend on the stiffness of the substructures and the deck. However, for simplicity, it is assumed that the vertical loads are uniformly distributed over the piers according to relevant tributary loading areas.

For the continuous deck on multiple supports, four combinations of pier heights are studied:

- 5 m–5 m–5 m;
- 10 m–10 m–10 m;
- 20 m–20 m–20 m;
- 5 m–10 m–5 m.

3.2. Deck Properties

The parametric analysis is performed considering five deck typologies typical of the Italian scenario [25].

The materials and geometry of the deck are defined based on the length of the spans. Specifically, for the simply supported scheme, three decks are considered:

- RC slab with four T beams, span 20 m;
- RC slab with three V beams, span 35 m;
- mixed section with two steel beams and a concrete slab, span 20 m;

While for the continuous deck scheme, the decks are

- RC slab with lightening tubes, span 20 m;
- RC box girder, span 35 m.

The assumed cross-sections are shown in Figure 8, while the assigned geometric and material properties and design loads are provided in Table 1.

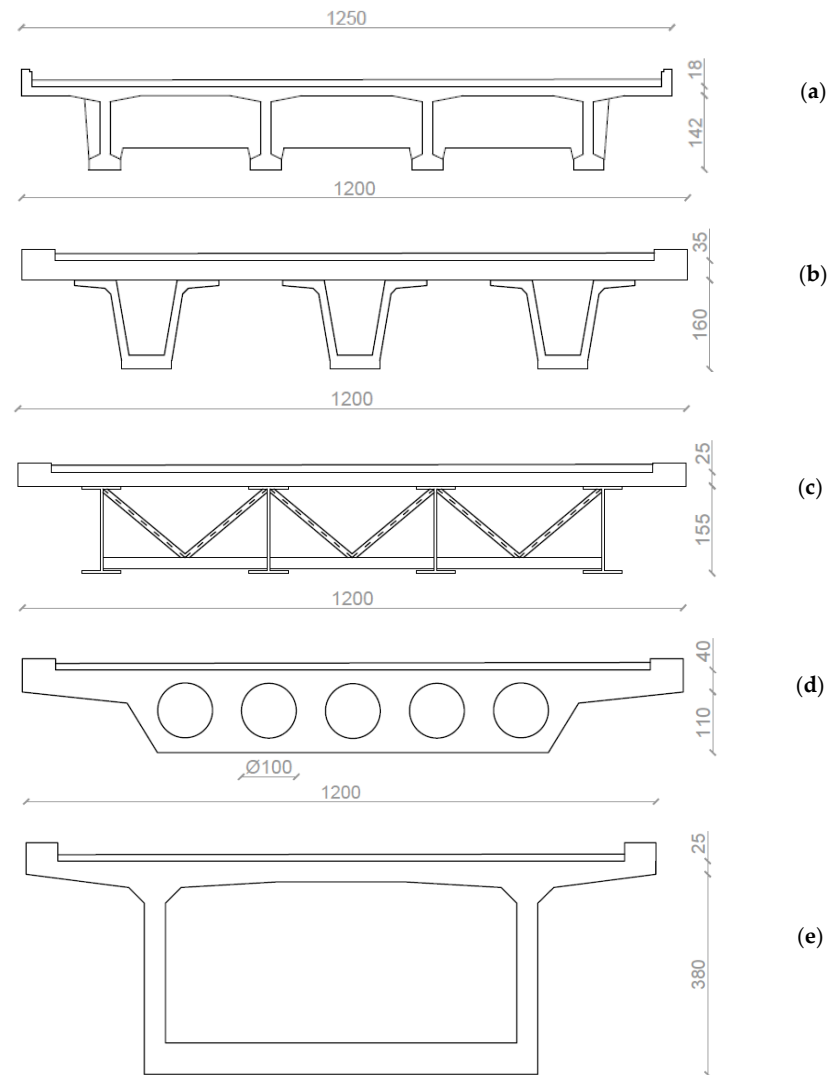


Figure 8. Deck cross-sections examined in the parametric study: (a) RC slab with T beams; (b) RC slab with V beams; (c) mixed deck; (d) RC slab with lightening tubes; (e) RC box girder. Measures in cm.

Table 1. Deck characteristics.

Property	Unit	RC Slab with T Beams	RC Slab with V Beams	Mixed Deck	RC Slab with Lightning Tubes	RC Box Girder
A_c	m^2	5.434	6.732	3.18	10.02	12.54
I_x	m^4	-	-	-	2.45	33.8
I_y	m^4	-	-	-	98.42	123.4
A_{beam}	m^2	-	-	0.57	-	-
A_{diaph}	m^2	-	-	0.072	-	-
γ_c	kN/m^3	25	25	25	25	25
γ_s	kN/m^3	-	-	78.5	-	-
g_1	kN/m	135.85	168.30	129.92	250.5	313.5
g_2	kN/m	47	47	47	47	47
L	m	20	35	20	20	35
G_{span}	kN	3657	7535.5	3538.3	-	-
G_{deck}	kN	-	-	-	23,800	50,470
Q_{span}	kN	1380	2190	1380	-	-
Q_{deck}	kN	-	-	-	4620	7860

A_c = area of concrete cross-section; I_x, I_y = area moment of inertia of deck cross-section (only for continuous deck); A_{beam} = area of steel beam cross-section; A_{diaph} = area of steel diaphragm cross-section; γ_c = concrete density; γ_s = steel density; g_1 = permanent structural load; g_2 = permanent non-structural load; L = span length; G_{span} = span weight (simply supported scheme); G_{deck} = deck weight (continuous deck scheme); Q_{span} = variable load on the single span (simply supported scheme); Q_{deck} = variable load on the deck (continuous deck scheme); “-”: not relevant/not applicable.

3.3. Pier Properties

Three types of RC piers, which reflect common typologies in Italian bridge heritage, are analyzed: the circular cross-section pier, the frame pier composed of three circular columns, and the hollow rectangular cross-section pier. The longitudinal reinforcement of the cross-section is modified as a function of the height, while the external dimensions of the cross-section are not changed.

Volumetric ratios of $\rho_s = 0.4\%$ and $\rho_w = 0.09\%$ (where ρ_s and ρ_w indicate the volume of the longitudinal steel bars divided by the volume of concrete and the volume of the stirrups divided by the volume of confined concrete, respectively) are assumed for the longitudinal and the transverse reinforcement of the 5 m high pier [26–28]. For the 10 m and 20 m high piers, the volumetric ratio counts are, respectively, $\rho_s = 0.7\%$ and $\rho_s = 1\%$, while the transverse volumetric ratio is $\rho_w = 0.09\%$, regardless of the pier height.

C25/30 concrete is assumed, with a Young’s modulus $E_c = 31,475.8$ MPa and a characteristic cylindrical strength $f_{ck} = 25$ MPa; the steel for the reinforcement is FeB44k, with a Young’s modulus $E_s = 200$ GPa, a characteristic yield strength $f_{yk} = 430$ MPa, and a characteristic tensile strength $f_{tk} = 540$ MPa.

3.3.1. Circular Cross-Section Pier

A cross-section of 2 m in diameter is considered, with the gross characteristics reported in Table 2. The longitudinal reinforcement is composed of 24 ϕ 26 bars (24 bars with diameter 26 mm) for the 5 m high pier, 32 ϕ 30 bars for the 10 m high pier, and 44 ϕ 26 bars for the 20 m high pier, respectively. The transversal reinforcement is made up, for all piers, of ϕ 16 circular stirrups with a spacing of 15 cm.

A sketch of the 5 m pier is shown in Figure 9. The dimensions of the pier cap are the same for the 10 m and 20 m piers.

Table 2. Circular cross-section pier: gross section characteristics.

Property	Unit	Value
D	m	2
A	m ²	3.142
I _x	m ⁴	0.785
I _y	m ⁴	0.785

D = pier diameter; A = pier cross-section area; I_x, I_y = area moment of inertia of the pier cross-section in x and y directions, respectively.

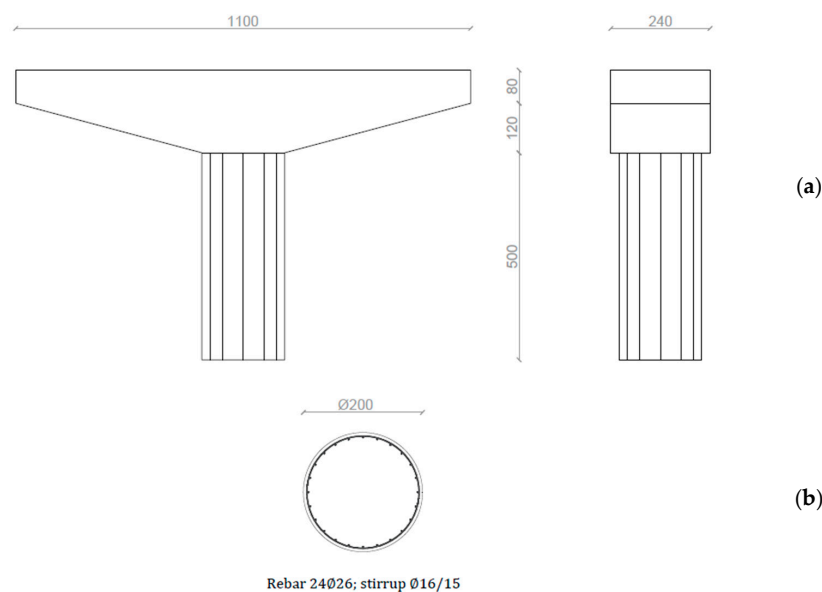


Figure 9. Circular cross-section pier: (a) elevation view; (b) cross-section with details of the reinforcement. Dimensions in cm.

3.3.2. Frame Pier

The frame pier consists of three cylindrical columns with a 1 m diameter each, connected at the top by a pier cap. Each column is reinforced with longitudinal bars arranged circumferentially and consisting, respectively, of 12 \varnothing 18 bars for the 5 m high pier, 12 \varnothing 24 bars for the 10 m high pier, and 17 \varnothing 24 bars for the 20 m high pier. The transversal reinforcement, regardless of the height of the column, is made up of \varnothing 10 circular stirrups with a spacing of 20 cm.

The gross section characteristics, valid for all heights, are shown in Table 3, while a sketch of the 5 m high pier is illustrated in Figure 10. The dimensions of the pier cap are the same for all heights.

Table 3. Frame pier: gross section characteristics.

Property	Unit	Value
D_c	m	1
A_c	m ²	0.785
I_x	m ⁴	0.15
I_y	m ⁴	28.52

D_c = column diameter; A_c = column cross-section area; I_x , I_y = area moment of inertia of the frame in x (longitudinal) and y (transversal) directions.

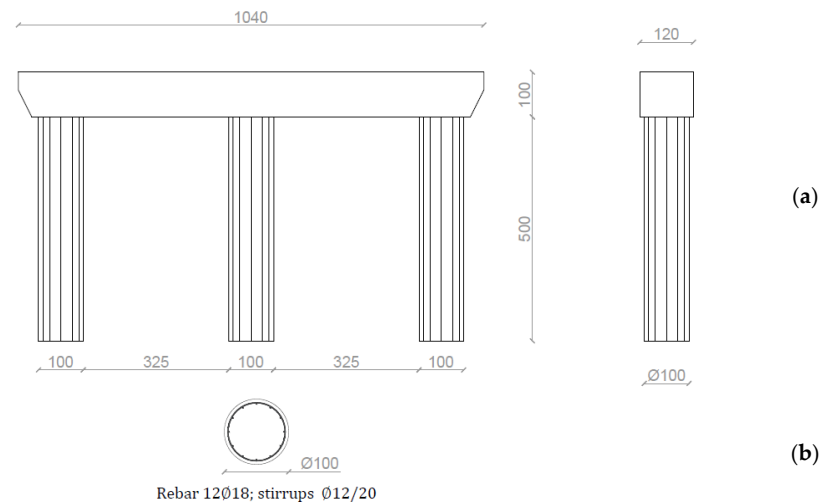


Figure 10. Frame pier: (a) elevation view; (b) cross-section with details of the reinforcement. Dimensions in cm.

3.3.3. Hollow Rectangular Cross-Section Pier

The hollow rectangular cross-section has a plan dimension of 5.5 m by 2 m; the thickness of the long sides is 30 cm, while that of the short sides is 40 cm. The longitudinal reinforcement consists, respectively, of 70 \varnothing 18 bars arranged along the perimeter of the cross-section for the 5 m high pier, 70 \varnothing 24 bars for the 10 m high pier, and 70 \varnothing 28 bars for the 20 m high pier, respectively. The transversal reinforcement is made up of 4 \varnothing 14 circular stirrups with a spacing of 15 cm.

The gross section characteristics, valid for all pier heights, are given in Table 4, and a sketch of the 5 m high pier is shown in Figure 11. The dimensions of the pier cap are the same for all heights.

Table 4. Hollow rectangular cross-section pier: gross section characteristics.

Property	Unit	Value
A	m ²	4.42
I_x	m ⁴	2.59
I_y	m ⁴	15.61

A = cross-section area; I_x , I_y = area moment of inertia of the cross-section in x and y directions.

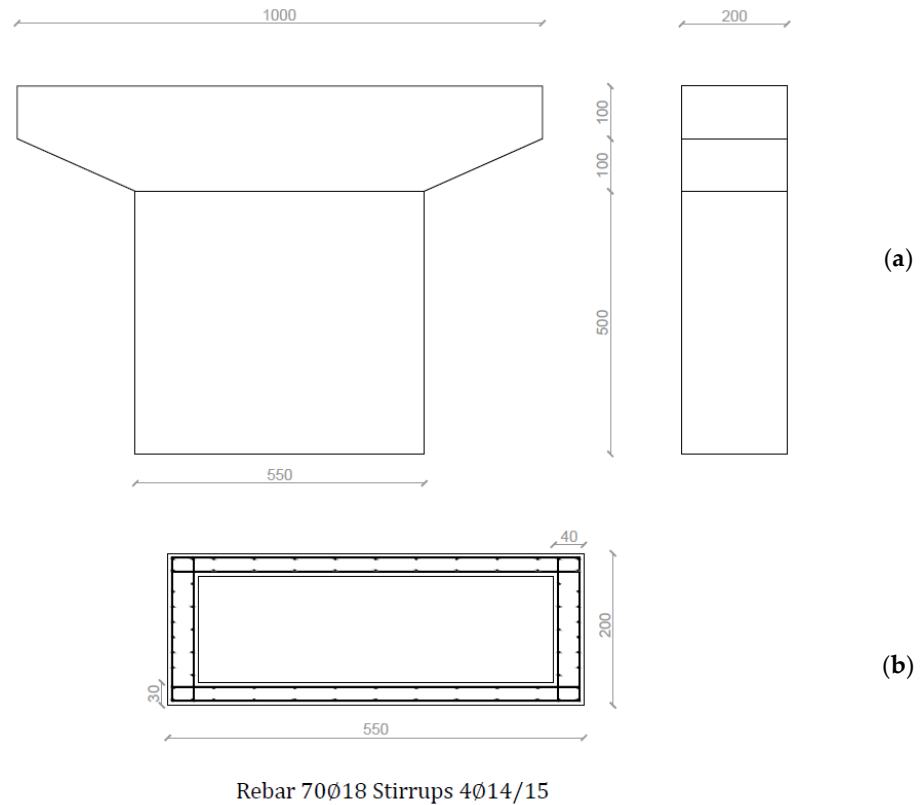


Figure 11. Hollow rectangular cross-section pier: (a) elevation view; (b) cross-section with details of the reinforcement. Dimensions in cm.

3.4. Design Seismic Action

The seismic action is defined according to IBC [20], assuming a design life $V_N = 50$ years and a use class IV ($c_u = 2.0$) (IBC, § 2.4.3), resulting in a reference period $V_R = V_N \cdot c_u = 100$ years (IBC, § 3.2.1). The performance of the bridge at the Life Safety Limit State is considered, corresponding to a return period of 949 years (IBC [20], § 3.2.1).

According to IBC [20], the Italian territory is divided into four zones based on the magnitude of horizontal peak ground acceleration (PGA), with a probability of exceedance equal to 10% in 50 years. Three seismic scenarios are examined, corresponding to seismic zones 1 (high), 2 (moderately high), and 3 (moderately low), and for each zone, a municipality is chosen: Reggio Calabria (PGA = 0.398 g) for zone 1; Sirmione (PGA = 0.241 g) for zone 2; and Pavia (PGA = 0.108 g) for zone 3. Topographic class T1 and soil type B are assumed for every site, resulting in the 5% damped spectra shown in Figure 12.

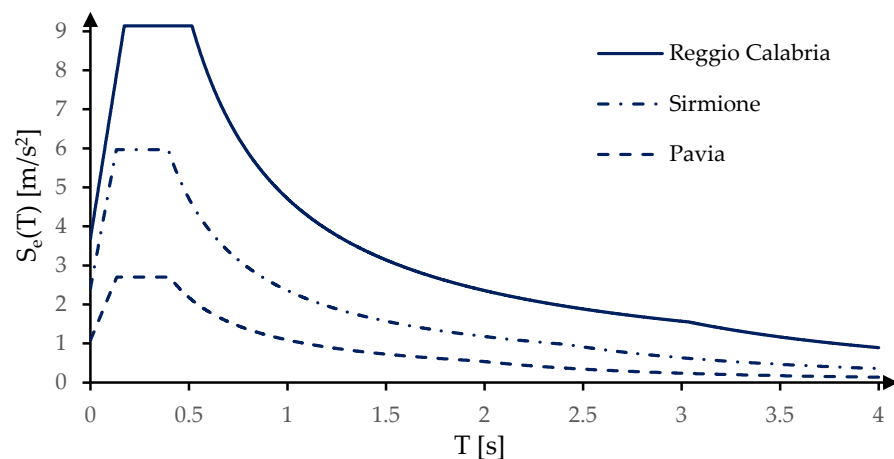


Figure 12. Design spectra for the three seismic scenarios.

4. Results

For the bridge prototypes described in Section 3, the effectiveness of deck isolation was assessed, combining the previously introduced material and geometrical characteristics with the seismic demand associated with the three seismic scenarios.

The first yield moment of the piers was calculated using the software program VCASTLU v.7.8 [29], which adopts the bending moment—curvature formulation of IBC [20], while the shear strength was calculated according to the recommendations of Chapter 6 of Eurocode 2 [30]. In the definition of both resistances, the axial load in the piers due to permanent loads and 20% of the variable traffic loads was taken into account. For the continuous deck scheme, the deck load was distributed on the piers based on their tributary loading areas; the accuracy and limits of such simplification will be discussed later.

By way of example, Table 5 shows the calculation flow for assessing the effectiveness of a bridge prototype characterized by the following properties:

- Static layout: simply supported span
- Type of deck: 20 m span, RC slab with T beams
- Pier section: circular, 2 m diameter
- Pier height: 5 m
- Seismic scenario: Zone 1, municipality of Reggio Calabria

Table 5. Example of suitability assessment.

Property	Symbol	Value	Unit
Pier axial load	N	5046	kN
Pier shear strength	V_{RD}	3151	kN
Pier yielding moment	M_y	5833	kNm
Effective mass	m_{eff}	515.8	ton
Elastic Limit acceleration	a_{EL}	2.26	m/s^2
Pier bending stiffness	K	593,305	kN/m
As-Built period	$T_{As\ Built}$	0.19	s
As-Built acceleration	$a_{As\ Built}$	9.14	m/s^2
Substructure mass	m_{sub}	114.9	ton
Substructure acceleration	a_{sub}	6.45	m/s^2
Equivalent Substructure acceleration	a_{ES}	1.44	m/s^2

The Elastic Limit acceleration ($2.26\ m/s^2$) is bracketed between the As-Built acceleration ($9.14\ m/s^2$) and the Equivalent Substructure acceleration ($1.44\ m/s^2$), revealing the effectiveness of deck isolation.

4.1. Simply Supported Deck Scheme

The results of the assessment for the simply supported decks are summarized in the matrix shown in Figure 13. For each seismic scenario, the deck type and pier height, the assessment may provide one of three outcomes: retrofit is not necessary (the elastic resource of the piers overcomes the seismic demand); retrofit is necessary and deck isolation is effective; or retrofit is necessary but deck isolation is not effective, as the seismic forces associated with the mass of the pier alone exceed the elastic resource of the latter).

The parametric study also allows for drawing some interesting conclusions regarding the effectiveness of deck isolation.

The pier with a circular cross-section requires the retrofit of the bridge in all seismic scenarios and for all heights, except in the case of tall piers (20 m high) in moderately low-seismicity areas. In this case, the flexibility of the piers lengthens the fundamental period of the bridge by reducing the As-Built acceleration below the Elastic Resource acceleration. The parametric analyses further reveal that in the high-seismicity zone, tall piers do not have sufficient elastic resources to resist the seismic forces associated with their own mass. In fact, in zone 1, only for the low pier (5 m high), the bending moment caused by the seismic force does not exceed the sectional resistance, and deck isolation is effective. On the contrary, in moderately high-seismicity zones, the isolation of the deck is always effective in protecting the piers.

Seismic zone	Deck	RC slab with T beams			RC slab with V beams			Mixed deck		
	Span	20 m			35 m			20 m		
	Pier height	5 m	10 m	20 m	5 m	10 m	20 m	5 m	10 m	20 m
1	Circular cross-section pier	Effective	Not effective	Not effective	Effective	Not effective	Not effective	Effective	Not effective	Not effective
	Frame pier	Effective	Not effective	Not effective	Effective	Not effective	Not effective	Effective	Not effective	Not effective
	Hollow rectangular cross-section pier	Effective	Effective	Not effective	Effective	Effective	Not effective	Effective	Effective	Not effective
2	Circular cross-section pier	Effective	Effective	Effective	Effective	Effective	Effective	Effective	Effective	Effective
	Frame pier	Effective	Not effective	Not effective	Effective	Effective	Effective	Effective	Not effective	Not effective
	Hollow rectangular cross-section pier	Effective	Effective	Effective	Effective	Effective	Effective	Effective	Effective	Effective
3	Circular cross-section pier	Effective	Effective	Not needed	Effective	Effective	Effective	Effective	Effective	Not needed
	Frame pier	Effective	Effective	Effective	Effective	Effective	Effective	Effective	Effective	Effective
	Hollow rectangular cross-section pier	Not needed	Effective	Not needed	Effective	Effective	Not needed	Not needed	Effective	Not needed

Not needed	Effective	Not effective
------------	-----------	---------------

Figure 13. Effectiveness matrix for simply supported deck scheme.

The frame pier is evaluated separately in the two horizontal directions of the bridge, since the pier has higher flexibility and lower strength in the longitudinal direction and higher stiffness and strength in the transverse direction. In this regard, the analyses highlight the intrinsic vulnerability of the pier due to its low capacity in the longitudinal direction. Bridge retrofit is always needed (at least in the weakest longitudinal direction), even in cases of moderately low seismicity. In the zones of high and moderately high seismicity, deck isolation is not effective for piers higher than 5 m but is effective for piers supporting the heavy RC deck with V beams in zone 2. The reduced vulnerability of the pier in this situation is an effect of the weight of the deck (the loads of the three simply supported decks are reported for reference in Table 1): heavy decks increase the axial compression of the pier and hence the bending capacity of the RC section.

The pier with a hollow rectangular cross-section was also evaluated separately in two principal horizontal directions due to its different inertial characteristics. It was found that seismic rehabilitation is necessary (at least in the weakest longitudinal direction) for all bridges and pier heights in high and moderately high seismicity zones, and in some cases in zone 3 (low or tall piers). Deck isolation is always effective except for tall (20 m) piers in seismic zone 1, thanks to the high elastic capacity of the hollow cross-section.

4.2. Continuous Deck Scheme

Figure 14 shows the results of the assessment of deck isolation applied to the continuous decks, according to the same template used in Figure 13.

The deck in RC slabs with lightening tubes requires retrofit for all types of piers, except for tall piers with a circular cross-section in a moderately low-seismicity area and for low or tall piers with a hollow rectangular cross-section. In fact, the analyses showed that tall piers have a sufficiently long fundamental period to reduce the As-Built acceleration below the Elastic Resource acceleration, and, on the other hand, in the short piers, the seismic force has a short lever arm, and the resulting base moment does not exceed the sectional strength of the pier.

Seismic zone	Deck	RC slab with lightning tubes				RC box girder			
	Span	20 m				35 m			
	Pier height	5-5 m	10-10 m	20-20 m	5-10 m	5-5 m	10-10 m	20-20 m	5-10 m
1	Circular cross-section pier	Effective	Not effective	Not effective	Not effective	Effective	Not effective	Not effective	Not effective
	Frame pier	Effective	Not effective	Not effective	Not effective	Effective	Effective	Not effective	Effective
	Hollow rectangular cross-section pier	Effective	Effective	Not effective	Effective	Effective	Effective	Not effective	Effective
2	Circular cross-section pier	Effective	Effective	Effective	Effective	Effective	Effective	Effective	Effective
	Frame pier	Effective	Effective	Not effective	Effective	Effective	Effective	Not effective	Effective
	Hollow rectangular cross-section pier	Effective	Effective	Effective	Effective	Effective	Effective	Effective	Effective
3	Circular cross-section pier	Effective	Effective	Not needed	Effective	Effective	Effective	Not needed	Effective
	Frame pier	Effective	Effective	Effective	Effective	Effective	Effective	Effective	Effective
	Hollow rectangular cross-section pier	Not needed	Effective	Not needed	Effective	Effective	Effective	Effective	Effective

Not needed	Effective	Not effective
------------	-----------	---------------

Figure 14. Effectiveness matrix for continuous deck scheme.

In zone 2, retrofitting is necessary for all piers but is not effective for tall frame piers due to their inherent weakness in the longitudinal bridge direction.

In the high-seismicity scenario, for circular cross-section piers and for frame piers, the deck isolation is effective only for low columns, since even for 10 m high piers, the base moment induced from the seismic force exceeds the sectional resistance. The hollow rectangular cross-section has a greater capacity, which allows the range of effectiveness to be extended to include 10 m piers. For the box girder deck, the upgrade is not necessary only for tall circular piers in the moderately low-seismicity zone 3, while with all other types of piers and seismic scenarios, the bridge requires a seismic rehabilitation. The suitability matrix is similar to that observed for the slab deck, except for the case of the deck with frame piers located in zone 1, for which deck isolation is also suitable for 10 m high piers instead of only for low piers. As already observed for simply supported decks, the effectiveness of deck isolation is increased in cases of heavy decks (the dead load of the box girder deck is more than twice the one of the RC slab deck; see Table 1) due to the beneficial effect of the axial compression on the bending capacity of the pier.

5. Discussion and Conclusions

A fast and easy-to-use tool for the preliminary assessment of the effectiveness of deck isolation for the seismic retrofit of existing bridges has been presented in this paper.

The retrofit procedure under consideration consists of replacing the existing bridge bearings with seismic isolators, creating an isolation layer between the deck and the substructures. The procedure is feasible for bridges characterized by a static scheme with simply supported spans or a continuous deck on multiple supports. The objective of the retrofit is to isolate the mass of the deck and reduce the seismic force on the substructures in order to avoid plasticization or brittle failure of the piers. This intervention is advantageous both in terms of reductions in time and, consequently, in interruptions of bridge service, and in terms of costs, comparable to and even lower than those of other conventional strategies, such as strengthening [31,32].

According to the procedure, two checks are performed: the first is that the piers are not able to resist the seismic force of the deck (need for retrofit), and the second is that

once the mass of the deck has been isolated, the piers are able to resist the seismic force associated with their own mass (effectiveness of deck isolation). If the second condition is not met, it is necessary to resort to alternative techniques, such as strengthening, or to the combination of deck isolation and pier strengthening. The procedure is characterized by an intrinsic simplicity, as it only requires performing an analysis of the pier section to calculate its capacity, which is then converted into the Elastic Resource acceleration and compared with the spectral acceleration of the bridge (As-Built acceleration) and with the normalized spectral acceleration of the pier alone (Equivalent Substructure acceleration). According to the procedure, the piers are analyzed separately, disregarding any coupling effects introduced by the isolators.

In the second part of the paper, a parametric study is presented to show a practical application of the method. The study covers some typical characteristics of Italian bridges, highlighting how some configurations are characterized by an intrinsic weakness and lack of substructure resources, which cannot be resolved by introducing an isolation layer below the deck, but it is also necessary to increase the strength of the weak element.

In particular, considering the simply supported deck scheme, the study reveals that seismic rehabilitation is always necessary to reduce the vulnerability of the piers, except for tall and flexible piers in bridges subjected to moderately low seismicity (zone 3 according to IBC [20]). However, it also emerges that circular section piers and frame piers are characterized by a serious structural deficiency if located in areas of high seismicity, as they are unable to resist the seismic force associated with their own mass. Rectangular hollow section piers perform better, and in this case, deck isolation is ineffective only in case of tall piers (20 m piers in the study). The high strength of the hollow rectangular section is also reflected by the fact that, in the case of moderately low seismicity, in many cases, the retrofit is not necessary at all.

Moving on to the continuous deck scheme, results similar to those of simply supported bridges are observed. For the circular section pier, it is found that retrofitting is always necessary, except for tall piers in zone 3, but isolation is not effective in cases of tall piers in zone 1. The intrinsic structural deficiencies of the frame pier are less evident than in the case of the simply supported deck. Finally, for piers with a hollow rectangular cross-section, the retrofit is necessary in most cases in seismic zone 3.

The parametric study also shows that the vulnerability of the piers is reduced as the dead load of the deck increases, thanks to the increase in the resistance of the RC section induced by the axial compression. This effect is evident when the frame pier is considered. In the simply supported scheme in zone 2, isolation is not effective for 10 m and 20 m high piers supporting 20 m long decks but becomes effective when the same piers support the 35 m long deck, whose dead load is approximately two times greater. Similarly, for the continuous deck scheme in seismic zone 1, the frame pier remains vulnerable after deck isolation when it is combined with the 20 m RC slab deck, but it is protected when it supports the 35 m box girder deck.

In the parametric study, for bridges with a continuous deck on multiple supports, for simplicity, a distribution of the deck mass on the piers based on the tributary loading area was used. This approach was validated, for the considered case studies, by comparing the results with those provided by a rigorous calculation of the vertical reactions based on the stiffness of the piers. The results of the comparison, reported in Appendix A, show that, for the examined bridge prototypes, the tributary area approach leads to underestimating—in general, by an amount between 5% and 15%—the axial load on the piers, which is conservative, since the elastic capacity of the RC sections of the piers increases with the increase in compression. Furthermore, the assessment was repeated considering the accurate reactions on the piers, obtaining a matrix of effectiveness practically equivalent to the one shown in Figure 14. Only in one case, where the a_{EL}/a_{ES} ratio was very close to unity, was a different outcome observed. However, in cases of continuous deck schemes with a more complex geometry than those considered in the study (which, it is worth recalling, represent common typologies of Italian bridges), when the “ a_{EL}/a_{ES} ” ratio is close to unity, the assumption of

uniform deck mass distribution may affect the result, providing a false positive or a false negative. To avoid this situation, in the application of the procedure, it is recommended, when the simplified mass distribution provides an " a_{EL}/a_{ES} " ratio between 0.95 and 1.05, to proceed according to the more rigorous approach that takes into account the stiffness of the structural elements.

As a final comment, it should be emphasized that, although some general conclusions of the parametric study can be extended to other types of bridges (in particular, bridges with short piers or with very tall piers with a long vibration period are expected to perform better during an earthquake), the results are not applicable to piers with different sections. Even for the RC piers examined in the study, the results depend on the steel reinforcement and therefore cannot be generalized, as the characteristics of the reinforcement strongly depend on the historical period of construction of the bridge. The collection of the geometric and material characteristics of the bridge components is therefore a fundamental step for the correct implementation of the procedure.

Although in the examples shown in the paper, the assessment procedure has been applied to some prototypes of RC bridges, in principle, it can be applied to any type of bridge that meets the requirement of having a deck totally supported by bridge bearings, regardless of the static scheme (simply supported spans or continuous deck) and the geometry and materials of the deck and the piers. It is therefore suitable for RC bridges, steel bridges, and composite bridges. In the opinion of the Authors, the proposed method can represent a practical tool for the assessment of bridges at the network scale. The criterion allows for performing an initial evaluation of the effectiveness of the deck isolation in a simple and fast way, avoiding in the preliminary phase time-consuming analyses which require the formulation of complex numerical models of the bridges. The method uses the equivalent static analysis, which is regularly used by the practitioners to perform the conceptual design of isolated structures, and therefore, its level of accuracy is aligned to current practice. It should indeed be borne in mind that the level of accuracy required for the assessment may depend on whether its purpose is to provide a refined assessment of a specific structure or to provide portfolio-scale predictions aimed at identifying potentially critical bridges that will be subjected to further in-depth analysis.

Author Contributions: Conceptualization, C.P.; methodology, C.P.; formal analysis, C.P.; data curation, C.P.; writing—original draft preparation, C.P.; writing—review and editing, V.Q.; visualization, C.P.; supervision, V.Q. All authors have read and agreed to the published version of the manuscript.

Funding: This research was funded by the Italian Department of Civil Protection (DPC) in the frame of the National Research Project DPC-ReLUIS 2022-2024 Work Package WP 15 "Contributi normativi a isolamento e dissipazione".

Institutional Review Board Statement: Not applicable.

Informed Consent Statement: Not applicable.

Data Availability Statement: Data is contained within the article.

Acknowledgments: The support of Regione Lombardia within the framework of the project "Analysis and monitoring of bridges and road structures" is gratefully acknowledged.

Conflicts of Interest: The authors declare no conflicts of interest.

Appendix A

To investigate the accuracy of the assumption of a distribution of the deck mass of continuous bridges based on the tributary loading area of the piers, the actual mass distribution of a continuous deck with four spans of the same length was calculated, taking account of the stiffness of its structural elements.

Finite element models of four bridges were formulated in SAP2000 v.19 software [33] using elastic beam elements for the deck and the piers, replicating the pier layouts (5–5–5 m; 10–10–10 m; 20–20–20 m; 5–10–5 m) examined in the parametric study. The geometric and

material properties defined in Table 1 (for the deck) and Tables 2–4 (for the piers) were assigned to the bridge elements in order to reproduce the characteristics of the bridges considered in Table 1. The elements were modeled without mass, and a distributed load on the deck was assigned according to Table 1. The lower end of the piers had fixed restraints; the abutments were modeled as hinges, and pinned connections were assumed between the piers and the deck.

The results of the analyses are shown in Figure A1 for the 20 m long RC slab deck with lightening tubes and in Figure A2 for the 35 m long RC box girder deck, respectively. The panels shown in the Figures report, for each pier type and pier layout, the ratio between the vertical reaction on the pier calculated by the finite element model and the vertical reaction according to the tributary area. Regardless of the type of deck and piers, the analyses reveal that the simplified mass distribution overestimates the vertical reactions on the abutments and underestimates the reactions on the two external piers. The accuracy of the simplified approach depends on the characteristics of the deck and of the piers, but the relative deviation in the vertical reactions for the two external piers P1 and P3 is, on average, between 5% and 15%. It is also interesting to note that the effect of piers of different heights, and therefore different stiffnesses, is evident only for continuous deck resting on circular cross-section piers.

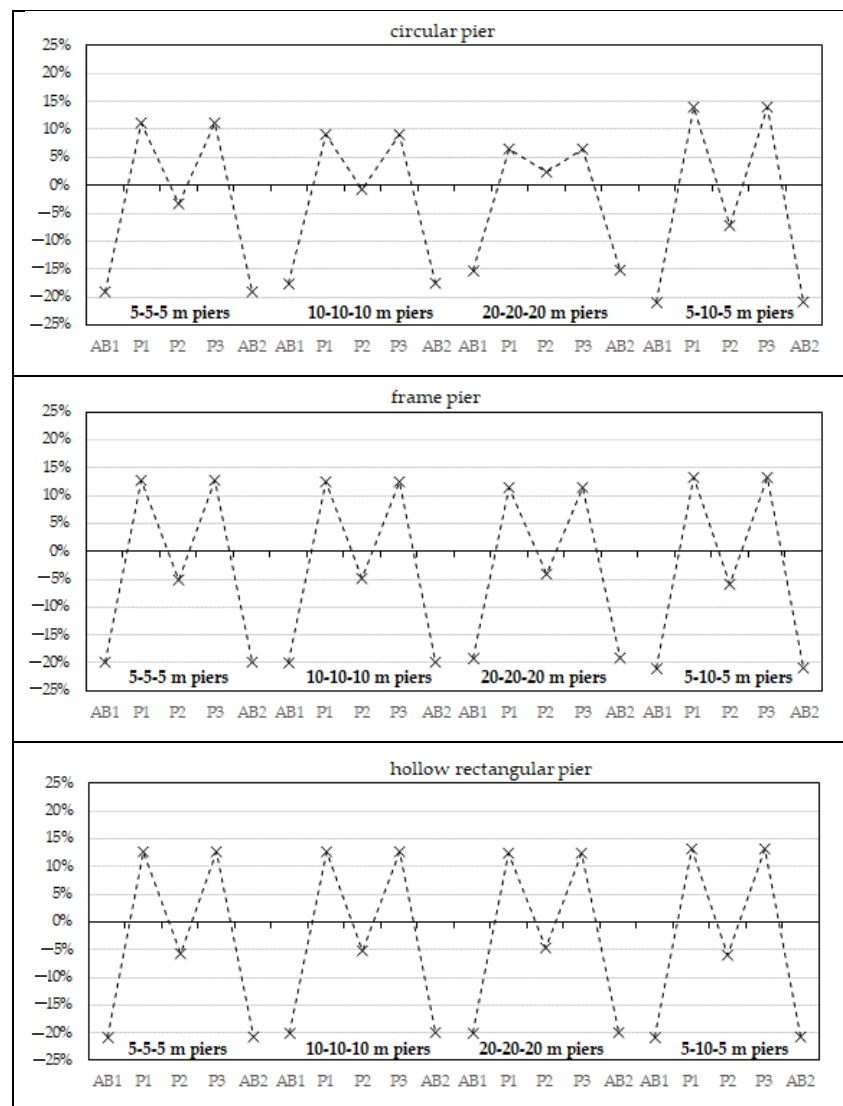


Figure A1. Continuous bridge with RC slab deck: change (in %) of pier vertical reactions considering the actual mass distribution in comparison to the simplified mass distribution based on the tributary loading area; AB1: Abutment 1; P1: Pier 1; P2: Pier 2; P3: Pier 3; AB2: Abutment 2.

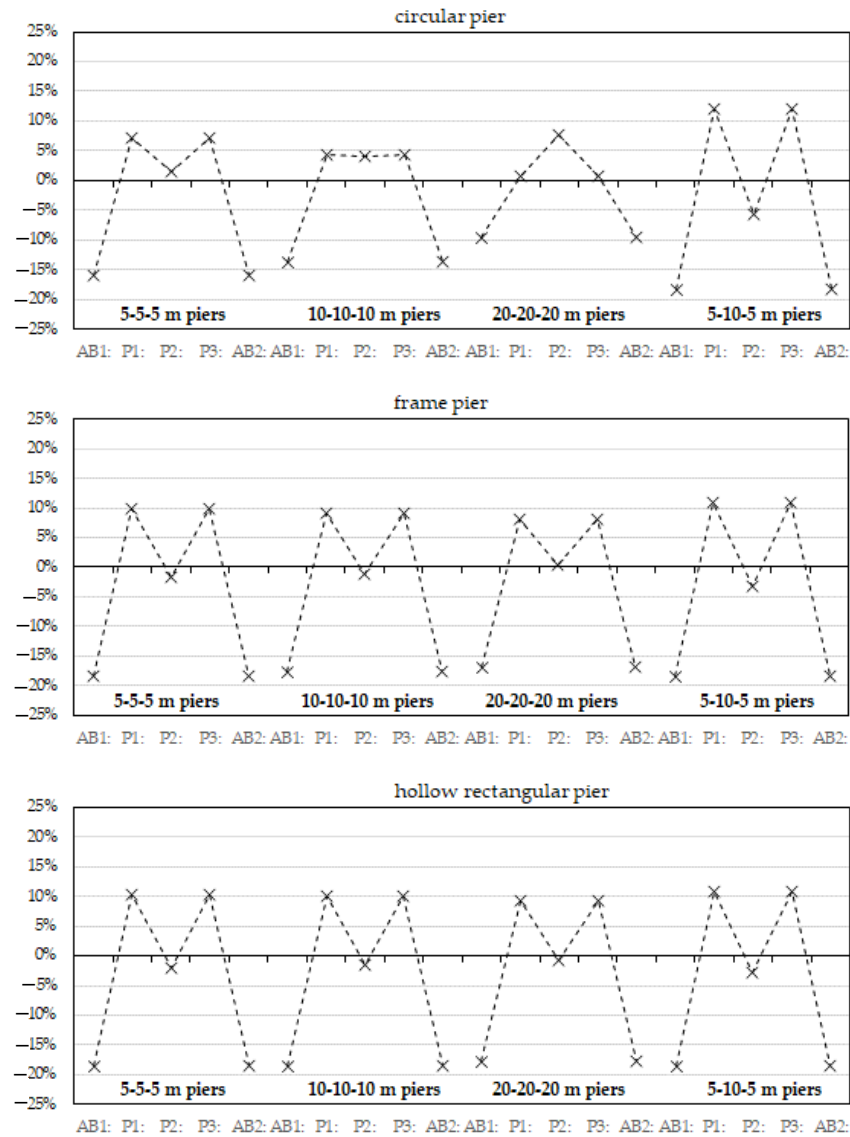


Figure A2. Continuous bridge with RC box girder deck: change (in %) of pier reactions considering the actual mass distribution in comparison to the simplified mass distribution based on the tributary loading areas; AB1: Abutment 1; P1: Pier 1; P2: Pier 2; P3: Pier 3; AB2: Abutment 2.

The effectiveness of deck isolation for the continuous deck bridges was assessed again by considering the vertical loads on the piers resulting from the actual mass distribution, providing the results shown in Figure A3. For the bridge with a 20 m RC slab deck the results are equivalent to those shown in Figure 14. For the bridge with a 35 m RC box girder deck the only difference concerns the case of the 10 m high pier with a circular section in zone 1: the deck isolation is found to be not effective if the simplified deck mass distribution is assumed but turns out to be effective by considering the more accurate vertical reactions, which give a 4% increase in the vertical load on every pier. As highlighted in the study, increasing the axial load on the piers has a beneficial effect, as it increases the capacity of the RC section. It is worth noting that in the only case where the accurate mass distribution provided a different result than the simplified distribution, the a_{EL}/a_{ES} ratio was very close to unity (0.988 for the simplified approach; 1.013 for the accurate approach).

Seismic zone	Deck	RC slab with lightning tubes				RC box girder			
	Span	20 m				35 m			
	Pier height	5-5-5 m	10-10-10 m	20-20-20 m	5-10-5 m	5-5-5 m	10-10-10 m	20-20-20 m	5-10-5 m
1	Circular cross-section pier	Effective	Not effective	Not effective	Not effective	Effective	Effective	Not effective	Not effective
	Frame pier	Effective	Not effective	Not effective	Not effective	Effective	Effective	Not effective	Effective
	Hollow rectangular cross-section pier	Effective	Effective	Not effective	Effective	Effective	Effective	Not effective	Effective
2	Circular cross-section pier	Effective	Effective	Effective	Effective	Effective	Effective	Effective	Effective
	Frame pier	Effective	Effective	Not effective	Effective	Effective	Effective	Not effective	Effective
	Hollow rectangular cross-section pier	Effective	Effective	Effective	Effective	Effective	Effective	Effective	Effective
3	Circular cross-section pier	Effective	Effective	Not needed	Effective	Effective	Effective	Not needed	Effective
	Frame pier	Effective	Effective	Effective	Effective	Effective	Effective	Effective	Effective
	Hollow rectangular cross-section pier	Not needed	Effective	Not needed	Effective	Effective	Effective	Effective	Effective

Not needed	Effective	Not effective
------------	-----------	---------------

Figure A3. Effectiveness matrix for continuous deck scheme considering the effective mass distribution on the piers.

References

- Calvi, G.M.; Pinho, R.; Magenes, G.; Bommer, J.J.; Restrepo-Vélez, L.F.; Crowley, H. Development of Seismic Vulnerability Assessment Methodologies over the Past 30 Years. *ISET J. Earthq. Technol.* **2006**, *43*, 75–104.
- Dolce, M.; Prota, A.; Borzi, B.; da Porto, F.; Lagomarsino, S.; Magenes, G.; Moroni, C.; Penna, A.; Polese, M.; Speranza, E.; et al. Seismic risk assessment of residential buildings in Italy. *Bull. Earthq. Eng.* **2021**, *19*, 2999–3032. [[CrossRef](#)]
- Micozzi, F.; Scozzese, F.; Ragni, L.; Dall'Asta, A. Seismic reliability of base isolated systems: Sensitivity to design choices. *Eng. Struct.* **2022**, *256*, 114056. [[CrossRef](#)]
- Franchin, P.; Baltzopoulos, G.; Biondini, F.; Callisto, L.; Capacci, L.; Carbonari, S.; Cardone, D.; Dall'Asta, A.; Flora, A.; Gorini, D.N.; et al. Seismic reliability of Italian code-conforming bridges. *Earthq. Eng. Struct. Dyn.* **2023**, *52*, 4442–4465. [[CrossRef](#)]
- Eröz, M.; DesRoches, R. Bridge seismic response as a function of the Friction Pendulum System (FPS) modeling assumptions. *Eng. Struct.* **2008**, *30*, 3204–3212. [[CrossRef](#)]
- Kawashima, K. Seismic isolation of highway bridges. *J. Jap. Ass. Earthq. Eng.* **2004**, *4–3*, 283–297. [[CrossRef](#)]
- Xiang, N.; Alam, M.S. Comparative seismic fragility assessment of an existing isolated continuous bridge retrofitted with different energy dissipation devices. *J. Bridge Eng.* **2019**, *24*, 04019070. [[CrossRef](#)]
- Bandini, P.A.C.; Siqueira, G.H.; Padgett, J.E.; Paultre, P. Seismic performance assessment of a retrofitted bridge with natural rubber isolators in cold weather environments using fragility surfaces. *J. Bridge Eng.* **2022**, *27*, 04022040. [[CrossRef](#)]
- Calvi, G.M.; Pavese, A. Conceptual design of isolation systems for bridge structures. *J. Earthq. Eng.* **1997**, *1*, 193–218. [[CrossRef](#)]
- Jara, M.; Casas, J.R. A direct displacement-based method for the seismic design of bridges on bi-linear isolation devices. *Eng. Struct.* **2006**, *28*, 869–879. [[CrossRef](#)]
- Dolce, M.; Cardone, D.; Palermo, G. Seismic isolation of bridges using isolation systems based on flat sliding bearings. *Bull. Earthq. Eng.* **2007**, *5*, 491–509. [[CrossRef](#)]
- Applied Technology Council. *ATC-40: Seismic Evaluation and Retrofit of Concrete Buildings*; Report No. SSC 96-01; Applied Technology Council: Redwood City, CA, USA, 1996.
- Cardone, D.; Dolce, M.; Palermo, G. Direct displacement-based design of seismically isolated bridges. *Bull. Earthq. Eng.* **2009**, *7*, 391–410. [[CrossRef](#)]
- Xie, Y.; Zhang, J. Design and optimization of seismic isolation and damping devices for highway bridges based on probabilistic repair cost ratio. *J. Struct. Eng.* **2018**, *144*, 04018125. [[CrossRef](#)]
- Furinghetti, M.; Pavese, A. Definition of a simplified design procedure of seismic isolation systems for bridges. *Struct. Eng. Int.* **2020**, *30*, 381–386. [[CrossRef](#)]

16. Guo, W.; Du, Q.; Huang, Z.; Gou, H.; Xie, X.; Li, Y. An improved equivalent energy-based design procedure for seismic isolation system of simply supported bridge in China's high-speed railway. *Soil Dyn. Earthq. Eng.* **2020**, *134*, 106–161. [[CrossRef](#)]
17. Gkatzogias, K.I.; Kappos, A.J. Deformation-based design of seismically isolated bridges. *Earthq. Eng. Struct. Dyn.* **2022**, *51*, 3243–3271. [[CrossRef](#)]
18. Pinto, P.E.; Franchin, P. Issues in the upgrade of Italian highway structures. *J. Earthq. Eng.* **2010**, *14*, 1221–1252. [[CrossRef](#)]
19. Borzi, B.; Ceresa, P.; Franchin, P.; Noto, F.; Calvi, G.M.; Pinto, P.E. Seismic vulnerability of the Italian roadway bridge stock. *Earthq. Spectra* **2015**, *31*, 2137–2161. [[CrossRef](#)]
20. Italian Council of Public Works. Technical Standards on Constructions. Italian Council of Public Works: Rome, Italy, 2018. (In Italian)
21. EN 1998-1; Eurocode 8: Design of Structures for Earthquake Resistance—Part 1: General Rules, Seismic Actions and Rules for Buildings. CEN European Committee for Standardization: Brussels, Belgium, 2004.
22. EN 1998-2; Design of Structures for Earthquake Resistance—Part 2: Bridges. CEN European Committee for Standardization: Brussels, Belgium, 2005.
23. Pettoruso, C. Strategies for the Rehabilitation of Existing Bridges by Seismic Isolation. Ph.D. Thesis, Politecnico di Milano, Milan, Italy, 2024.
24. Italian Railway Agency. *Manuale di Progettazione Delle Opere Civili Parte II: Ponti e Strutture*; Italian Railway Agency: Rome, Italy, 2020. (In Italian)
25. Angotti, F. (Ed.) *Dettagli Costruttivi di Strutture in Calcestruzzo Armato*; AICAP Italian Association for Structural Concrete: Rome, Italy, 2011. (In Italian)
26. Pinto, A.V.; Molina, J.; Tsionis, G. Cyclic tests on large-scale models of existing bridge piers with rectangular hollow cross-section. *Earthq. Eng. Struct. Dyn.* **2003**, *32*, 1995–2012. [[CrossRef](#)]
27. Pettoruso, C.; Quaglioni, V. Comparison of Linear and Nonlinear Procedures for the Analysis of the Seismic Performance of Straight Multi-Span RC Bridges. *Buildings* **2024**, *14*, 464. [[CrossRef](#)]
28. Delgado, R.; Delgado, P.; Pouca, N.V.; Arede, A.; Rocha, P.; Costa, A. Shear effects on hollow section piers under seismic actions: Experimental and numerical analysis. *Bull. Earthq. Eng.* **2009**, *7*, 377–389. [[CrossRef](#)]
29. Gelfi, P. Verifica Cemento Armato allo Stato Limite Ultimo (VCASLU). Available online: https://gelfi.unibs.it/software/programmi_studenti.html (accessed on 6 June 2024).
30. EN 1992-1-1; Eurocode 2: Design of Concrete Structures—Part 1-1: General Rules and Rules for Buildings. CEN European Committee for Standardization: Brussels, Belgium, 2004.
31. Dicleli, M.; Mansour, M.Y. Seismic retrofitting of highway bridges in Illinois using friction pendulum seismic isolation bearings and modeling procedures. *Eng. Struct.* **2003**, *25*, 1139–1156. [[CrossRef](#)]
32. Dicleli, M.; Mansour, M.Y.; Constantinou, M.C. Efficiency of seismic isolation for seismic retrofitting of heavy substructure bridges. *J. Bridge Eng.* **2005**, *10*, 429–441. [[CrossRef](#)]
33. Computers & Structures Inc. *SAP 2000 CSI Analysis Reference Manual*; Computers & Structures Inc.: Berkeley, CA, USA, 2016.

Disclaimer/Publisher's Note: The statements, opinions and data contained in all publications are solely those of the individual author(s) and contributor(s) and not of MDPI and/or the editor(s). MDPI and/or the editor(s) disclaim responsibility for any injury to people or property resulting from any ideas, methods, instructions or products referred to in the content.